

Quinazoline Sulfonamides as Dual Binders of the Proteins B-Cell Lymphoma 2 and B-Cell Lymphoma Extra Long with Potent Proapoptotic Cell-Based Activity

Brad E. Sleebs,^{†,‡} Peter E. Czabotar,^{†,‡} Wayne J. Fairbrother,[§] W. Douglas Fairlie,^{†,‡} John A. Flygare,[§] David C. S. Huang,^{†,‡} Wilhelmus J. A. Kersten,^{†,‡} Michael F. T. Koehler,[§] Guillaume Lessene,^{†,‡} Kym Lowes,^{†,‡} John P. Parisot,^{†,‡} Brian J. Smith,^{†,‡} Morey L. Smith,^{||} Andrew J. Souers,^{||} Ian P. Street,^{†,‡} Hong Yang,^{†,‡} and Jonathan B. Baell^{*,†,‡}

[†]The Walter and Eliza Hall Institute of Medical Research, 1G Royal Parade, Parkville, Victoria 3052, Australia

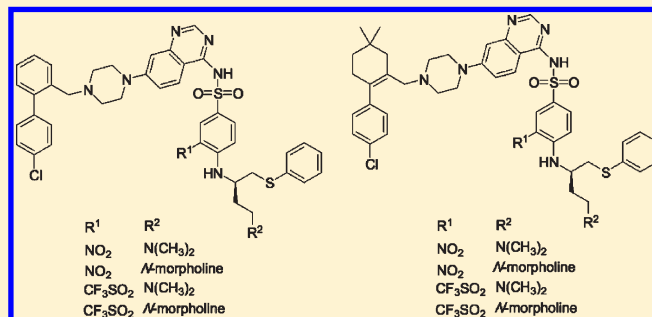
[‡]Department of Medical Biology, University of Melbourne, Parkville, Victoria 3010, Australia

[§]Departments of Discovery Chemistry and Protein Engineering, Genentech, Inc. 1 DNA Way, South San Francisco, California 94080, United States

^{||}Cancer Research, Global Pharmaceutical Research and Development, Abbott Laboratories, 100 Abbott Park Road, Abbott Park, Illinois 60064, United States

S Supporting Information

ABSTRACT: ABT-737 and ABT-263 are potent inhibitors of the BH3 antiapoptotic proteins, Bcl-x_L and Bcl-2. This class of putative anticancer agents invariably contains an acylsulfonamide core. We have designed and synthesized a series of novel quinazoline-based inhibitors of Bcl-2 and Bcl-x_L that contain a heterocyclic alternative to the acylsulfonamide. These compounds exhibit submicromolar, mechanism-based activity in human small-cell lung carcinoma cell lines in the presence of 10% human serum. This comprises the first successful demonstration of a quinazoline sulfonamide core serving as an effective benzoylsulfonamide bioisostere. Additionally, these novel quinazolines comprise only the second known class of Bcl-2 family



protein inhibitors to induce mechanism-based cell death.

■ INTRODUCTION

B-cell lymphoma 2 (Bcl-2) family proteins comprise two classes with diametrically opposed functions—those that are prosurvival and those that are proapoptotic—and their interplay modulates the balance between cell survival and cell death.¹ Prosurvival proteins include Bcl-2, B-cell lymphoma extra long (Bcl-x_L), B-cell lymphoma w (Bcl-w), myeloid cell leukemia 1 (Mcl-1), and B-cell lymphoma 2 related protein A1 (A1), and these lie upstream of the pro-apoptotic proteins Bcl-2 associated protein X (Bax) and Bcl-2 antagonist/killer (Bak), which mediate cell death through permeabilization of the mitochondrial outer membrane. This results in liberation of cytochrome c (and other apoptogenic factors) into the cytosol, which activates the caspase cascade en route to apoptosis. Despite their opposing functions, all members of this protein family are structurally related, possessing four Bcl-2 homology (BH) motifs: BH1, BH2, BH3, and BH4. Prosurvival proteins bind to Bax and Bak, thus neutralizing their ability to induce cell death. This brake can be released when an upstream subclass of proapoptotic proteins, called the BH3-only proteins, bind to prosurvival proteins. The BH3-only proteins include Bcl-2-associated death promotor (Bad), BH3 interacting death domain (Bid), Bcl-2

interacting killer (Bik), Bcl-2 interacting mediator (Bim), Bcl-2 modifying factor (Bmf), Harakiri-Bcl-2 interacting protein (Hrk), phorbol-12-myristate-13-acetate-induced protein 1 (Noxa), and Bcl-2 binding component 3 (Puma) and are upregulated in response to various cellular stresses (e.g., DNA damage, growth factor deprivation). Unlike Bax/Bak and the prosurvival proteins that adopt a well-defined, conserved helical-bundle three-dimensional structure, the BH3 only proteins (which are so-called because they possess only the BH3 motif), are intrinsically unstructured,² with the exception of Bid.

Dysfunctional apoptosis is a hallmark of most, if not all, cancers as it allows damaged cells that would otherwise be removed to survive and, in some cases, proliferate.³ Various conventional anticancer chemo- and radiotherapy treatment regimes work by up-regulating BH3-only proteins to trigger apoptosis in tumor cells, and their effectiveness is often blunted by the overexpression of prosurvival proteins, a common apoptotic defect in many cancers.^{4,5} In addition, their efficacy is also diminished by upstream defects in the pathway, such as

Received: December 15, 2010

Published: March 02, 2011

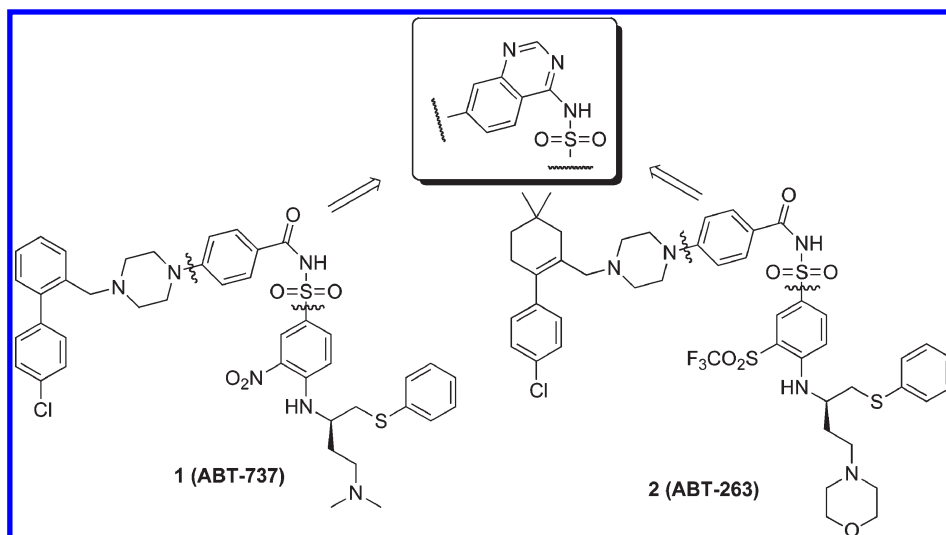


Figure 1. Structures of known BH3 mimetics with pro-apoptotic activity, acylsulfonamides **1** and **2**, and the proposed quinazoline isosteric scaffold (boxed).

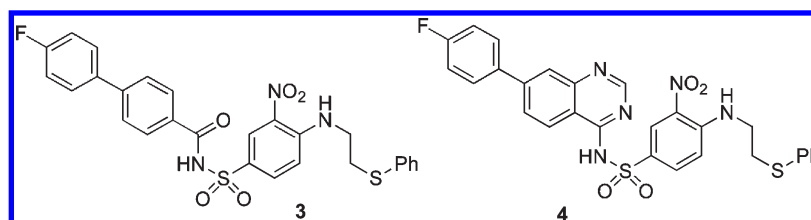


Figure 2. Structures of 4-fluorobiaryl compound **3** and the targeted model quinazoline sulfonamide **4**.

inactivating mutations of p53 (found in ~50% of all human cancers), which is required for transcriptional up-regulation of prodeath proteins Puma and Noxa in response to these DNA-damaging insults. Small-molecule mimetics of BH3-only proteins could potentially overcome both of these issues by neutralizing the prosurvival proteins present, even when they are produced in excess, allowing for the release of Bax/Bak and ensuing apoptosis in a manner that bypasses the need for activation of p53.⁶

Intense interest in small-molecule BH3 mimetics is reflected in numerous recent publications. However, demonstration of mechanism-based induction of apoptosis has generally not been reported.^{6–8} An exception is the acylsulfonamide series of inhibitors from Abbott Laboratories, exemplified by **1** (ABT-737, Figure 1), which was reported to inhibit Bcl-x_L, Bcl-2, and Bcl-w with an IC₅₀ of less than 1 nM, greater than 3 orders of magnitude more potently than previously described small-molecule inhibitors.⁹ This compound exhibited single-agent mechanism-based killing of lymphoma and small cell lung carcinoma (SCLC) cell lines as well as primary patient-derived chronic lymphocytic leukemia cells. In murine xenograft models, **1** improved survival, caused regression of established tumors, and produced cures in a high percentage of the animals. A related compound, **2** (Navitoclax or ABT-263, Figure 1), was subsequently prepared that demonstrates oral availability across multiple species, and that has now entered phase II clinical trials.^{10,11}

A hallmark of all members of this class of drugs is the presence of an acylsulfonamide core. This moiety represents a potential metabolic liability and indeed has been used in prodrug approaches for sulfonamides where the acyl group is cleaved in vivo.¹² For this reason, we felt that there would be considerable

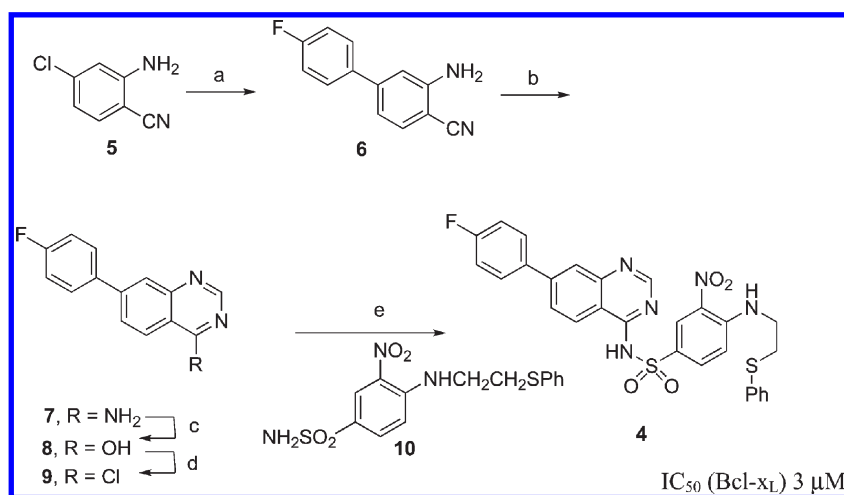
interest in the identification of an isosteric replacement of the acylsulfonamide. We postulated that a quinazoline sulfonamide may serve such a purpose while being topographically appropriate to maintain high affinity binding to Bcl-2 family proteins. Herein, we report the synthesis of a series of quinazoline sulfonamides, their binding affinities for Bcl-x_L and Bcl-2, and their mechanism-based cell killing activity.

RESULTS AND DISCUSSION

To explore the utility of the quinazoline isostere, we first undertook the synthesis of a compound based on acylsulfonamide **3** (Figure 2). Compound **3** is an early generation Bcl-x_L inhibitor¹³ from Abbott that served as a starting point for the generation of **1**. We reasoned that the demonstration of adequate binding to Bcl-x_L by quinazoline isostere **4** would substantiate the more intensive synthesis required for the quinazoline-based surrogates of **1**.

As shown in Scheme 1, synthesis of **4** was initiated via Suzuki coupling of 2-amino-4-chlorobenzonitrile with 4-fluorophenylboronic acid to afford intermediate **6** in an unoptimized yield of 56%. The formation of quinazoline **7** was then accomplished through condensation with formamidine acetate at 120 °C. Acid-mediated hydrolysis followed by chlorination afforded the 4-chloroquinazoline **9**, which was then coupled with sulfonamide **10**¹³ to afford the quinazoline sulfonamide **4** in good yield.¹⁴

The affinities of compounds **3** and **4** for Bcl-x_L were then determined via an amplified luminescent proximity homogeneous assay (AlphaSCREEN), based on competition between test compound and Bim for Bcl-x_L, affording IC₅₀ values of 1.5

Scheme 1. Synthesis of the 4-Fluorophenylquinazoline Sulfonamide **4**^a

^a Reagents and conditions: (a) 4-Fluorophenylboronic acid, K₂CO₃, TBAB, Nájera's catalyst, TBAB, K₂CO₃, reflux, 2 h [water] 56%. (b) Formamidine acetate, MeOCH₂CH₂OH, 120 °C, 5 h, 75%. (c) 5 N aqueous HCl, reflux, 30 min, 92%. (d) SOCl₂, CHCl₃, cat. DMF, 99%. (e) DMF, K₂CO₃, 85 °C, 68%.

and 3 μM, respectively. This result provided initial validation of the quinazoline design and prompted the synthesis of the more elaborate quinazoline-bearing analogue of **1** (**21**, Scheme 2). As shown in Scheme 2, regioselective nitro displacement of 2,4-dinitrobenzonitrile with *N*-Boc piperazine and subsequent acid-mediated deprotection afforded intermediate **13**, which was then alkylated with 2-bromomethylbromobenzene to furnish **14**. The 4-chlorobenzene moiety was then installed via Suzuki coupling conditions to afford intermediate **15**. Iron-mediated nitro-reduction followed by quinazoline formation as described afforded **17**. Subsequent hydrolysis of the 4-amino group and chlorination using thionyl chloride furnished the desired 4-chloroquinazoline **19** in high overall yield. Finally, base-mediated coupling with sulfonamide **20**¹⁵ afforded the desired target **21** after HPLC purification.

In the AlphaSCREEN competition assay, quinazoline **21** returned an IC₅₀ against Bcl-x_L of 3 nM, as compared with that for **1** of 1 nM (data not shown). To determine binding constants, surface plasmon resonance (SPR) studies were undertaken, and the results are shown in Figure 3a for **21**, along with those for **1** in Figure 3b. The binding kinetics of **21** and **1** were characterized by extremely slow dissociation rates and returned kinetic *K_D* values of 4.2 and 0.37 nM, respectively, in broad agreement with the AlphaSCREEN competition assay data. As can be observed in Figure 3a, compound **21** exhibits a slightly decreased association rate and increased dissociation rate as compared with **1** (Figure 3b), explaining the slight decrease in overall binding affinity. By comparison, the 26-mer Bim BH3 peptide exhibits a binding constant of 28 pM and is therefore 150-fold more potent than compound **21**, a result of both extremely high association and slow dissociation rates (data not shown).

We then assessed the selectivity profile of **21** against a panel of Bcl-2 prosurvival family proteins using an SPR-based solution competition assay. As demonstrated in Table 1, **21** is a potent, dual Bcl-x_L/Bcl-2 competitive ligand with no measured affinity for Mcl-1. This binding profile of **21** with respect to Bcl-2 and Bcl-x_L is similar to **1**, while in contrast, the affinity of **21** for Bcl-w is significantly less (~10-fold higher IC₅₀) than **1**.

To investigate the binding interactions of **21** with Bcl-x_L, a complex was crystallized, and the structure determined to 2.0 Å

resolution (Figure 4a,b). As demonstrated in Figure 4b, **21** binds to Bcl-x_L in a manner similar to **1**^{9,16} with a high degree of overlap between the two molecules. The chlorophenyl group of both compounds projects identically and deeply into the P2 hydrophobic pocket, and the phenylthio-tethered phenylsulfonamide similarly occupies the P4 hydrophobic pocket. Notably, however, an electrostatic interaction between the quinazoline endocyclic nitrogen atom in the 1 position and the hydroxyl group of Tyr101 is evident (Figure 4b), providing an additional specific point of contact that is not observed in the corresponding complex of **1** and Bcl-x_L.

To induce apoptosis in wild-type mouse embryonic fibroblasts (MEFs), both Bcl-x_L and Mcl-1 must be neutralized.¹⁷ Acylsulfonamide **1** has low affinity for Mcl-1 and thus fails to induce apoptosis in cell lines expressing this protein. Therefore, to investigate cell-based activity, wild-type (*mcl-1*^{fl/fl}) or Mcl-1-deficient (*mcl-1*^{-/-}) mouse MEFs were treated with varying concentrations of either **1** or quinazoline **21** in the presence of 10% fetal bovine serum (Figure 5). Both **1** and quinazoline **21** potently killed MEFs lacking Mcl-1, with respective EC₅₀ values of 51 and 110 nM. However, they were much less potent against wild-type MEFs, and **21** returned an EC₅₀ of 5.8 μM, while **1** did not show appreciable cytotoxicity even at the highest dose tested (10 μM). This selectivity for inducing apoptosis in Mcl-1-deficient but not wild-type MEFs is consistent with the high affinity of these compounds for Bcl-x_L but not Mcl-1. This is an important observation because such evidence of mechanism-based cellular activity in other reported BH3 mimetics is generally lacking. Indeed, where tested, other reported BH3 mimetics appear to induce cell killing in a nonspecific manner.⁸ The quinazoline system reported here therefore represents only the second known class of Bcl-2 family protein inhibitors shown to induce mechanism-based cell death.

In the course of this work, a subsequent series of publications by Abbott Laboratories detailed the synthesis and characterization of a related Bcl-2/Bcl-x_L inhibitor, **2** (Figure 1). These publications reported that distinct modular changes allowed for retention of mechanism-based cell killing via Bcl-2 family member inhibition while conferring enhanced oral bioavailability in preclinical species. Specifically, the modifications included the

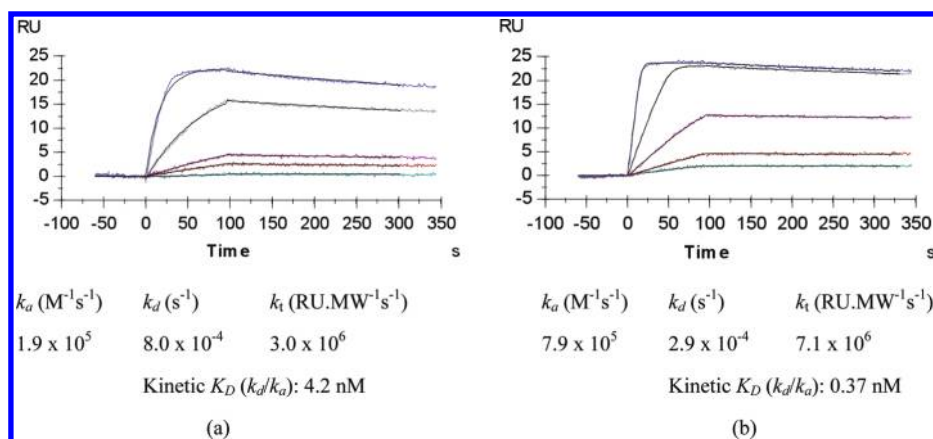
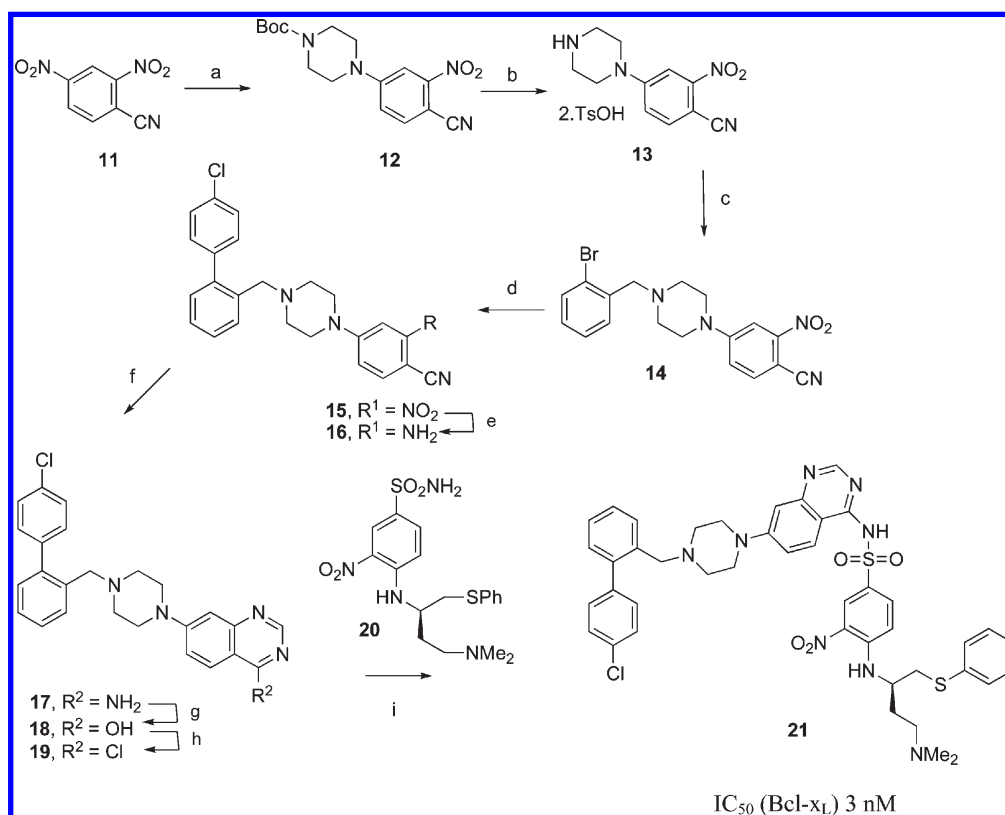


Figure 3. SPR study of (a) quinazoline **21** and (b) **1** with Bcl- x_L . Representative sensorgrams for direct binding assays were performed on the Biacore S51 with **1** (injections of 270, 90, 30, 10, and 3.3 nM) and **21** (injections of 500, 125, 31.25, 7.8, and 1.95 nM). The fine black line over each colored sensorgram is the fit (one-to-one binding with mass transport limitations) provided by the Biacore S51 Evaluation Version 1.2.1 data analysis software. Sensorgrams are characterized in both cases by extremely slow off-rates as observed in the trace from $T = 100$ s onward. Listed for each sensorgram are the derived k_a , k_d , k_t (mass transport constant: RU are response units, and MW is molecular mass in Dalton), and kinetic K_D . All values are $\pm 50\%$.

Scheme 2. Synthesis of the Elaborated Quinazoline Sulfonamide **21**^a



^a Reagents and conditions: (a) *N*-Boc-piperazine, DMSO, 25 °C, 72 h, 56%. (b) TsOH, 2 h [MeCN], 83%. (c) 2-Bromobenzyl bromide, Et₃N [iPrOH], 93%. (d) 4-Chlorophenylboronic acid, PdCl₂(PPh₃)₂, Na₂CO₃, [DME/EtOH/H₂O], 81%. (e) Fe 60 °C, 40 min, [AcOH], 85%. (f) Formamidine acetate, MeOCH₂CH₂OH, 120 °C, 6 h, 81%. (g) AcOH, concentrated HCl, 130 °C, 9 h. (h) SOCl₂, CHCl₃, cat DMF, 12 h, 80%. (i) DMF, K₂CO₃, 85 °C.

saturation of the western biphenyl group, replacement of the nitro moiety with a trifluoromethylsulfonyl group, and variation of the eastern basic amine tail. These reports prompted us to target the synthesis of a discrete set of additional quinazoline-based isosteres shown in Figure 6.

The modular synthesis of these analogues allowed for the initial preparation of the quinazoline core, followed by the appropriate incorporation of building blocks described previously by the Abbott group.^{10,15,18} To this end, **12** was reduced and converted to the amino quinazoline **36** in high yield by

treatment with formamidine acetate (Scheme 3). Acid hydrolysis of the Boc protecting group followed by alkylation of the piperazine **24** with halide synthons **22** and **23** proceeded smoothly to afford **18** and **37**, respectively.

Table 1. Selectivity Profile of **1** and Quinazoline **21** for Bcl-2 Family Members as Assessed by a Biacore 3000 Competition Assay^a

compd	IC ₅₀ (nM)			
	Bcl-x _L	Bcl-2	Bcl-w	Mcl-1
1	<3 ^b	6.1	40	>1000
21	7	8.7	440	>1000

^aIC₅₀ values (±50%) were determined by solution competition assays. An 11-point 2-fold dilution series of each compound was incubated with recombinant pro-survival proteins and percentage bound determined by SPR using a Biacore 3000 instrument with a wild-type mBimBH3 (DLRPEIRIAQELRRIGDEFNETYTRR) peptide immobilized on the SPR chip. ^bBelow the lower limit of the measurement range for this assay.

Chlorination of these 4-hydroxyquinazolines proved troublesome, and purification could not be performed on silica chromatography without significant degradation. However, the use of optimized reaction conditions followed by purification via alumina chromatography returned good yields of target products **19** and **38**. The coupling reactions of the various sulfonamide fragments with the corresponding chloroquinazoline intermediates also proved difficult as initial attempts with various bases were generally low yielding and produced multiple byproducts. A number of temperature and solvent variations were also attempted, and it was found that addition of a catalytic amount of copper(I) iodide and palladium tetrakis(triphenylphosphine) had a marked effect on the coupling. Employing this modification in conjunction with microwave irradiation at 150 °C afforded all eight desired quinazolines **21** and **28–34** in excellent yields (Scheme 3).

All compounds were tested for binding affinity for Bcl-2 family members and cell-killing activity in wild-type (*mcl-1*^{fl/fl}) or Mcl-1-deficient (*mcl-1*^{-/-}) MEFs in both 1 and 10% serum (Table 2).

As shown in Table 2, quinazolines **21**, **29**, **31**, and **33** were particularly potent Bcl-x_L/Bcl-2 dual inhibitors with IC₅₀ values

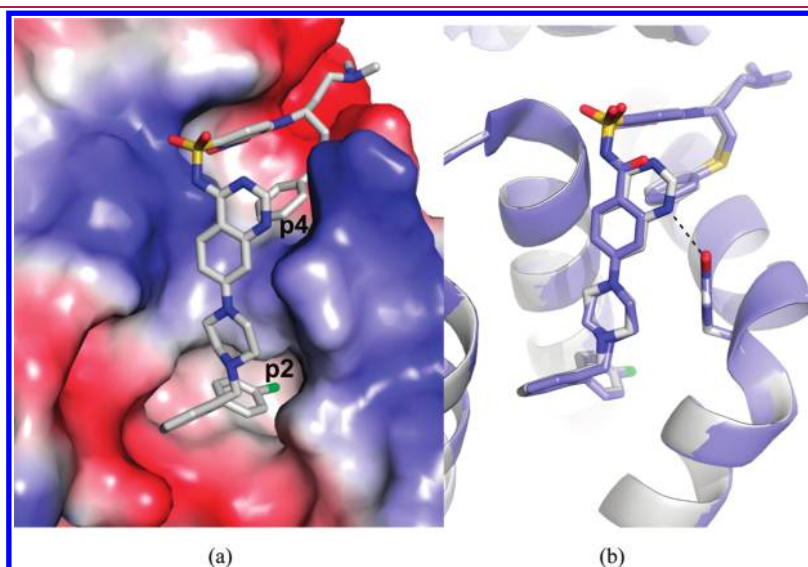


Figure 4. (a) Complex of quinazoline **21** with Bcl-x_L, showing the electrostatic molecular surface with hydrophobic pockets P2 and P4 labeled as shown. (b) Overlay of the compound **21** complex (white) with the complex of Bcl-x_L and **1** (blue). A hydrogen bond between the quinazoline nitrogen and the hydroxyl group of Tyr101 on Bcl-x_L (N–O distance 2.60 Å) is apparent. This figure was created using PyMol.

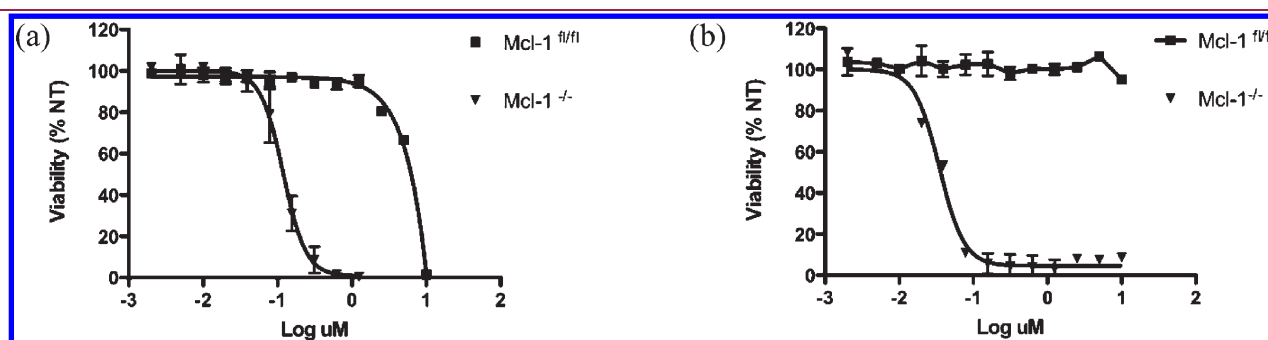


Figure 5. Viability of wild-type (*mcl-1*^{fl/fl}) and Mcl-1-deficient (*mcl-1*^{-/-}) MEFs 24 h after treatment with (a) quinazoline **21** or (b) **1**, in the presence of 10% fetal bovine serum. Means ± SEMs of a representative of three experiments.

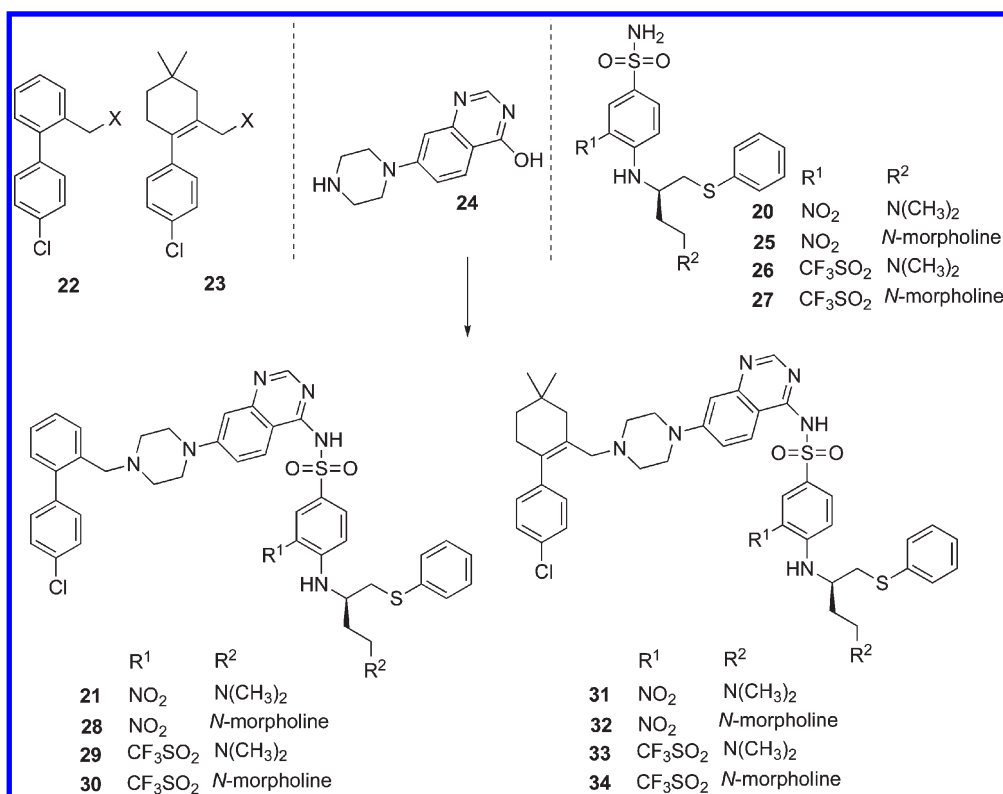
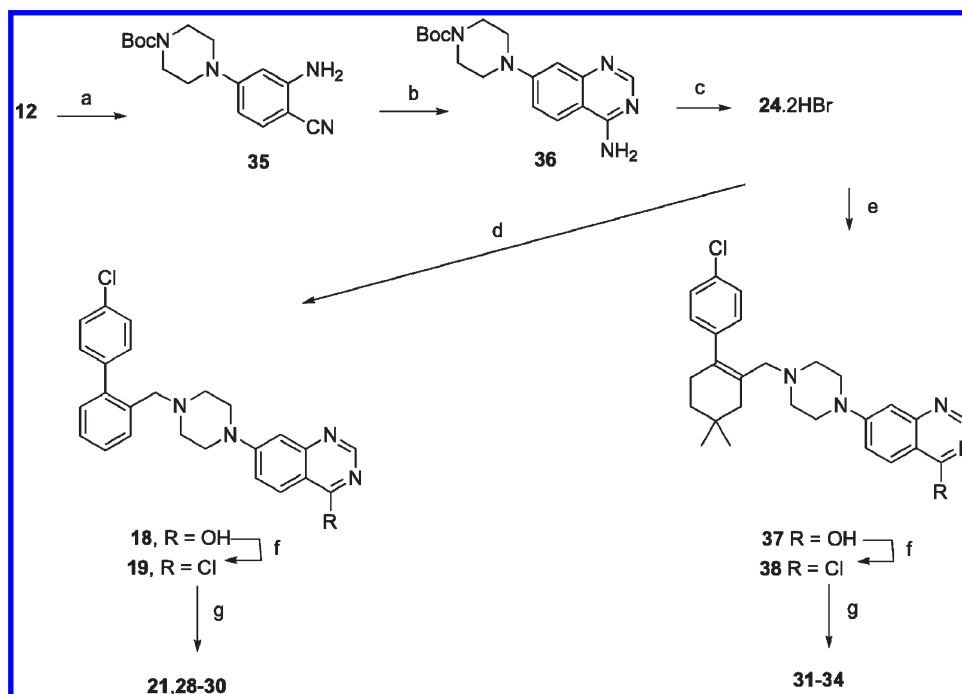


Figure 6. Targeted quinazoline sulfonamides and proposed convergent synthesis.

Scheme 3. Synthesis of Hydroxyquinazoline Core and Alkylation with Alkyl Halides^a



^a Reagents and conditions: (a) Fe, AcOH, 60 °C, 45 min. (b) Formamidine acetate, MeOCH₂CH₂OH, 120 °C, 6 h. (c) 6 N HBr, 130 °C, 3 h. (d) Compound 22 (X = Br), DIPEA, DMF, 25 °C, 20 h. (e) Compound 23 (X = Cl), DIPEA, DMF, 25 °C, 20 h. (f) POCl₃, cat. DMF, DCE, 70 °C, 20 h. (g) Cs₂CO₃, CuI, Pd(PPh₃)₄, dioxane, μ W, 150 °C, 45 min, with appropriate sulfonamide coupling partner.

of less than 15 nM for both proteins. The least active quinazoline was 34 with respective IC₅₀ values of 29 and 84 nM, while the

activities of remaining compounds 28, 30, and 32 lay within the range spanned by 21 and 34. All compounds exhibited weaker

Table 2. Activity of Quinazolines against Bcl-2 Family Members and in MEFs

compd	IC ₅₀ (nM) ^a				cellular EC ₅₀ (nM) ^b			
	Bcl-x _L	Bcl-2	Bcl-w	Mcl-1	mcl-1 ^{fl/fl} (1% serum)	mcl-1 ^{fl/fl} (10% serum)	mcl-1 ^{-/-} (1% serum)	mcl-1 ^{-/-} (10% serum)
21	7	9	440	>1000	1680	5820	40 ± 11	110 ± 13
28	34	21	>1000	>1000	>10000	>10000	24.8 ± 4.7	190 ± 25
29	6	13	245	>1000	c	c	c	c
30	16	81	>1000	>1000	>10000	>10000	22.4 ± 2.5	149 ± 20
31	3	12	540	>1000	1610	4300	16.0 ± 9.8	61 ± 11
32	20	21	>1000	>1000	>10000	>10000	38 ± 13	221.6 ± 7.1
33	3	5	275	>1000	2650	5460	11.6 ± 6.9	37.2 ± 3.2
34	29	84	>1000	>1000	>10000	>10000	37.2 ± 6.2	328 ± 34
1	3	6.1	40	>1000	>10000	>10000	2.03 ± 0.37	51 ± 11

^aIC₅₀ values (±50%) were determined by solution competition assays. An 11-point 2-fold dilution series of each compound was incubated with recombinant pro-survival proteins and percentage bound determined by SPR using a Biacore 3000 instrument with a wild-type mBimBH3 (DLRPEIRIAQELRRIGDEFNETYTRR) peptide immobilized on the SPR chip. ^bMEFs were treated with compound for 24 h, and cytotoxicity was assessed by CellTiter Glo assay. Cellular EC₅₀ represents the range of compound concentration in which cell viability was reduced by 50% as compared to no treatment control. Data represents means ± SEMs for three independent experiments. ^cNot tested.

Table 3. Activity of Quinazolines in Cancer Cells (SCLC)

compd	SCLC activity (EC ₅₀ , μM) in 10% human serum ^a		
	H146	H889	H1963
21	0.61	0.21	0.17
28	3.7	1.3	1.4
30	0.63	0.82	0.40
31	0.54	0.41	0.17
32	1.2	0.60	0.46
33	0.71	0.72	0.30
34	1.1	1.6	0.71
2	0.080	0.12	0.051

^aCells were treated for 48 h in 96-well tissue culture plates in medium supplemented with 10% human serum. Cell viability was assessed using an MTS proliferation assay. All values represent the average from single experiments run in triplicate (±50%).

activity against Bcl-w and no activity against Mcl-1. Consistent with the latter finding, the quinazoline analogues were essentially inactive when tested against wild-type MEFs in concentrations of up to 10 μM. Where EC₅₀ values could be derived, these were in the micromolar range, and we attribute this activity to nonspecific cytotoxicity. In stark contrast, all quinazolines were much more potent against Mcl-1-deficient MEFs, even in the presence of 10% serum. Here, the weakest compound was **34**, with an EC₅₀ for 328 nM, while **33** was considerably more potent and, with an EC₅₀ of 37 nM, was essentially equipotent to **1**. This correlates with the respective Bcl-x_L/Bcl-2 inhibition by these two compounds in the competition assays, and indeed, the data in Table 2 show that this trend is remarkably consistent across the set of quinazolines tested. As also shown in Table 2, all compounds were more potent by 3- (**21**) to 9- (**34**) fold when tested in the presence of only 1% serum.

These compounds were then assessed for their ability to induce cell killing in a panel of SCLC cell lines known to be highly sensitive to acylsulfonamides **1** and **2**. As shown in Table 3, quinazolines **21**, **30**, **31**, and **33** were potent even in the presence of 10% human serum, with submicromolar EC₅₀ values across the three SCLC cell lines tested. Compounds **28**, **32**, and **34** were

marginally less potent. However, **2** was substantially more potent than the quinazolines and registered EC₅₀ values of between 51 and 120 nM for the three different SCLC cell lines.

CONCLUSIONS

Acylsulfonamides **1** and **2** are high-affinity inhibitors of Bcl-2 and Bcl-x_L and show potent cell killing in cell lines that are dependent on these proteins for viability. Here, we have discovered that the benzoylsulfonamide portion of these compounds can be replaced by a quinazolinesulfonamide scaffold to furnish a new class of Bcl-2 family inhibitors. Like the acylsulfonamides, these quinazoline sulfonamides exhibit low nanomolar activity against Bcl-2 and Bcl-x_L but no activity toward Mcl-1. There are some differences in the Bcl-2 family selectivity profile between these two compound classes, however, and unlike the acylsulfonamides, the quinazolines are significantly weaker against Bcl-w as compared with Bcl-x_L and Bcl-2. X-ray crystallographic analysis of quinazoline **21** in complex with Bcl-x_L shows a binding mode very similar to acylsulfonamide **1**, with the exception that the nitrogen atom in the 1 position of the quinazoline ring forms an additional electrostatic interaction with the hydroxyl group of Tyr101 in Bcl-x_L. This observation is notable in that the corresponding interaction is not possible with **1**; yet, its affinity for Bcl-x_L is several times higher than the affinity of quinazoline **21** for Bcl-x_L.¹⁹

Significantly, these quinazolines produce potent and mechanism-based cytotoxicity in MEFs where Mcl-1 has been genetically silenced. They also exhibit submicromolar activity against a panel of small-cell lung carcinoma cell lines in the presence of 10% human serum. After the acylsulfonamides, these compounds comprise the only known class of functional BH3 mimetics that confer mechanism-based cell killing.

EXPERIMENTAL SECTION

Chemistry. *General Chemistry Methods.* All nonaqueous reactions were performed in oven-dried glassware under an atmosphere of dry nitrogen, unless otherwise specified. Tetrahydrofuran was freshly distilled from sodium/benzophenone under N₂. Dichloromethane was freshly distilled from CaH₂ under N₂. All other solvents were reagent grade. Petroleum ether describes a mixture of hexanes in the bp range

40–60 °C. Analytical thin-layer chromatography was performed on Merck silica gel 60F₂₅₄ aluminum-backed plates and were visualized by fluorescence quenching under UV light. Flash chromatography was performed with silica gel 60 (particle size 0.040–0.063 mm). NMR spectra were recorded on a Bruker Avance DRX 300 with the solvents indicated (¹H NMR at 300 MHz). Chemical shifts are reported in ppm on the δ scale and referenced to the appropriate solvent peak. NMR spectra for compounds **21** and **28–34** were recorded on a Bruker 500 MHz NMR spectrometer and referenced to tetramethylsilane. The analysis for total nitrogen, carbon, hydrogen, and sulfur was determined by Dr. Thomas Rodemann at the Central Science Laboratory, University of Tasmania, using a Thermo Finnigan EA 1112 Series Flash Elemental Analyzer. HRESMS were recorded at the Australian National University Mass Spectrometry Facility using a Waters LCT Premier XE (ESI TOF Mass Spectrometer). Preparative HPLC was performed on a Polaris C18 5 μ m column (50 mm \times 21 mm). Low-resolution mass spectra were performed on a Finnigan LCQ Advantage MAX or recorded on a Sciex 15 mass spectrometer in ES⁺ mode. Purity analysis of final compounds was performed on a Berger Instruments SFC system operating at 100 bar, 35 °C, column) Berger diol, 4.6–150 mm, with a 6 min gradient of 20–60% MeOH in CO₂ flowing at 2.35 mL/min (SFCd method) or a Berger pyridine column, 4.6–150 mm, with a 6 min gradient of 5–50% MeOH in CO₂ flowing at 2.35 mL/min (SFCp). All final compounds were analyzed using ultrahigh performance liquid chromatography/ultraviolet/evaporative light scattering detection coupled to time-of-flight mass spectrometry (UHPLC/UV/ELSD/TOFMS). Unless otherwise noted, all tested compounds were found to be >95% pure by this method.

Chemistry Experimental. *3-Amino-4'-fluorobiphenyl-4-carbonitrile (6).* 2-Amino-4-chlorobenzonitrile (608 mg, 4 mmol), 4-fluorophenylboronic acid (834 mg, 6 mmol), K₂CO₃ (1.10 g, 8 mmol), TBAB (1.28 g, 4 mmol), and Nájera's catalyst²⁰ (2.5 mol %) in water (15 mL) were refluxed in air for 2 h, and the product was extracted with warm toluene (4 \times 20 mL). The organic layer was separated, dried (MgSO₄), and decanted through a silica plug, eluting product with CH₂Cl₂. The crude product was recrystallized from 50% cyclohexane/toluene to give the biaryl **6** as an off-white solid (480 mg, 56%). ¹H NMR (DMSO-*d*₆): δ 7.64–7.59 (2H, m), 7.44 (1H, dd, *J* = 8.2 and 1.2 Hz), 7.32–7.26 (2H, m), 7.01 (1H, s), 6.85–6.82 (1H, m), 6.08 (2H, bs). HRESMS found: (M + H) 213.0833; C₁₃H₉FN₂ requires (M + H), 213.0823.

7-(4-Fluorophenyl)-4-aminoquinazoline (7). To the biaryl **6** (212 mg, 1 mmol) in ethylene glycol monomethyl ether (2 mL) was added formamidine acetate (360 mg, 6 mmol), and the mixture was refluxed under nitrogen for 5 h. The mixture was cooled, and the product was filtered off to give the quinazoline **7** as colorless plates (180 mg, 75%). ¹H NMR (DMSO-*d*₆): δ 8.38 (1H, s), 8.26 (1H, d, *J* = 8.6 Hz), 7.74–7.87 (6H, m), 7.31 (2H, m). Anal. found: C, 69.82; H, 3.90; N, 17.54; C₁₄H₁₀FN₃ requires C, 70.28; H, 4.21; N, 17.56%.

7-(4-Fluorophenyl)-4-hydroxyquinazoline (8). The 4-amino-quinazoline **7** (85 mg, 0.36 mmol) in 5 N HCl (5 mL) was heated to reflux for 30 min, and the solution was allowed to cool; on standing, a precipitate formed, which was filtered off and washed with water to give quinazolinone **8** as a white solid (78 mg, 92%). ¹H NMR (DMSO-*d*₆): δ 8.20 (1H, s), 8.17 (1H, dd, *J* = 8.31 and 0.5 Hz), 7.89–7.80 (4H, m), 7.37–7.31 (2H, m). Anal. found: C, 69.68; H, 4.00; N, 11.56; C₁₄H₉FN₂O requires C, 69.99; H, 3.78; N, 11.66%.

7-(4-Fluorophenyl)-4-chloroquinazoline (9). The quinazolinone **8** (103 mg, 0.43 mmol) in anhydrous CHCl₃ (1 mL) and SOCl₂ (1 mL) with 1 drop of DMF was heated to reflux for 30 min. Ice water was added, and the mixture was extracted with EtOAc (2 \times 10 mL). The organic layer was dried (MgSO₄) and evaporated in vacuo to yield the 4-chloroquinazoline **9** as a creamy solid (110 mg, 99%). This sample was on-reacted without further purification or characterization.

N-(7-[4-Fluorophenyl]quinazolin-4-yl)-4-(phenylthio)ethan-2-ylamino)-3-nitro benzenesulfonamide (4). A mixture of the crude 4-chloroquinazoline **9** (26 mg, 0.1 mmol), the sulfonamide **10** (35 mg, 0.1 mmol), and K₂CO₃ (138 mg, 1.0 mmol) in DMF (1 mL) was heated at 60 °C for 24 h. A 10% citric acid solution (8 mL) was added, and the solution was extracted with EtOAc (2 \times 10 mL). The organic layer was then dried (MgSO₄) and concentrated in vacuo to give a yellow solid. The solid was then triturated with hot toluene (2 \times 2 mL) and then CH₃CN (2 \times 2 mL) to give the sulfonamide **4** as a yellow powder (39 mg, 68%). HRESMS found: (M + H) 576.1170; C₂₈H₂₂FN₅O₄S₂ requires (M + H), 576.1170. ¹H NMR (DMSO-*d*₆): δ 8.63 (1H, m), 8.59 (1H, d, *J* = 2.0 Hz), 8.41 (1H, bs), 8.23 (1H, d, *J* = 8.4 Hz), 7.79–7.96 (5H, m), 7.07–7.40 (9H, m), 3.56–3.63 (2H, m), 3.21–3.28 (2H, m).

tert-Butyl 4-(4-Cyano-3-nitrophenyl)piperazine-1-carboxylate (12). A mixture of 2,4-dinitrobenzonitrile (10 g, 51.8 mmol) and *N*-Boc-piperazine (19.2 g, 103.6 mmol) in DMSO (60 mL) was stirred for 3 days at 25 °C. The dark brown reaction mixture was then partitioned between EtOAc (400 mL) and water (2 \times 100 mL). The layers were separated, and the organic layer was dried (MgSO₄) and concentrated under vacuum. The resulting residue was triturated with Et₂O and filtered to give the nitrile **12** as a deep yellow powder (8 g, 47%). A second crop was obtained from the supernatant on standing after some evaporation had taken place (1.7 g, 10%). HRESMS found: (M + H) 333.1536; C₁₆H₂₀N₄O₄ requires (M + H), 333.1537. ¹H NMR (CDCl₃): δ 7.69–7.04 (2H, m), 7.05 (1H, dd, *J* = 2.7 and 8.8 Hz), 3.65–3.61 (4H, m), 3.49–3.43 (4H, m), 1.49 (9H, s).

2-Nitro-4-(piperazin-1-yl)benzonitrile Bistosylate (13). The piperazine **12** (8.64 g, 15 mmol) and *p*-toluenesulfonic acid (12.9 g, 75 mmol) were dissolved in CH₃CN (60 mL) and left to stand for 2 h. The product in the form of a bis-tosylate **13** was then filtered off as coarse prisms (7.2 g, 83%). M⁺ [ES⁺] 233. ¹H NMR (DMSO-*d*₆): δ 8.80 (1H, bs), 7.88 (1H, d, *J* = 8.82 Hz), 7.76 (1H, d, *J* = 2.58 Hz), 7.46 (4H, d, *J* = 8.07 Hz), 7.37 (1H, dd, *J* = 8.82 and 2.58 Hz), 7.09 (4H, d, *J* = 8.07 Hz), 3.6–3.7 (4H, m), 3.1–3.3 (4H, m), 2.25 (6H, s). Anal. found: C, 50.35; H, 5.12; N, 9.22; S, 10.42; C₂₅H₂₈N₄O₈S₂·H₂O requires C, 50.49; H, 5.08; N, 9.42; S, 10.78%.

4-(4-(2-Bromobenzyl)piperazin-1-yl)-2-nitrobenzonitrile (14). To the bis-tosylate **13** (2.3 g, 4.0 mmol) and 2-bromobenzylbromide (1.49 g, 6.0 mmol) in *i*-PrOH (15 mL) was added Et₃N (1.95 mL, 14.0 mmol), and the whole was stirred for 3 h. MeOH (20 mL) was then added, the mixture was allowed to stand a few minutes, and the aryl bromide product **14** was filtered off pure as an orange powder (1.5 g, 93%). M⁺ [ES⁺] 401, 403. ¹H NMR (DMSO-*d*₆): δ 7.80 (1H, d, *J* = 8.9 Hz), 7.67, d, *J* = 2.47 Hz), 7.58 (1H, d, *J* = 7.6 Hz), 7.49 (1H, d, *J* = 7.6 Hz), 7.36 (1H, dd, *J* = 7.6 and 7.6 Hz), 7.30 (1H, dd, *J* = 8.9 and 2.47 Hz), 7.19 (1H, dd, *J* = 7.6 and 7.6 Hz), 3.58 (2H, s), 3.4–3.5 (4H, m), 2.5–2.6 (4H, m). Anal. found: C, 53.92; H, 4.50; N, 13.95; S, 10.42; C₁₈H₁₇BrN₄O₂ requires C, 53.88; H, 4.27; N, 13.96%.

4-(4-(4'-Chlorobiphenyl-2-yl)methyl)piperazin-1-yl)-2-nitrobenzonitrile Tosylate (15). A mixture of the aryl bromide **14** (1.38 g, 3.43 mmol), *p*-chlorophenylboronic acid (703 mg, 4.46 mmol), sodium carbonate (763 mg, 7.2 mmol), and PdCl₂(PPh₃)₂ (5 mol %) in a mixture of DME (6 mL), EtOH (6 mL), and water (6 mL) was heated at 90 °C for 4 h under an atmosphere of nitrogen. The reaction mixture was partitioned between EtOAc and water and filtered through Celite, and the organic layer was dried (MgSO₄) and evaporated in vacuo. The resulting residue was then treated with *p*-toluenesulfonic acid (1.72 g, 10 mmol) in CH₃CN (20 mL) and Et₂O (40 mL). On standing in the freezer, the nitroarene product **15** precipitated as a yellow powder (1.68 g, 81%). M⁺ [ES⁺] 433, 435. ¹H NMR (DMSO-*d*₆): δ 9.57 (1H, bs), 7.85 (1H, d, *J* = 8.8 Hz), 7.7–7.8 (1H, m), 7.69 (1H, d, *J* = 2.52 Hz), 7.4–7.6 (6H, m), 7.2–7.4 (4H, m), 7.08 (2H, d, *J* = 7.9 Hz), 4.36 (2H, m), 4.07 (2H, m), 3.22 (4H, m), 2.88 (2H, m), 2.25 (3H, s). Anal. found:

C, 59.47; H, 4.99; N, 8.89; S, 4.94; $C_{31}H_{29}ClN_4O_5S \cdot H_2O$ requires C, 59.75; H, 5.01; N, 8.99; S, 5.15%.

2-Amino-4-(4-(4'-chlorobiphenyl-2-yl)methyl)piperazin-1-yl)benzonitrile (**16**). The nitroarene tosylate **15** (1.3 g, 2.15 mmol) and iron powder (1.1 g, 19.4 mmol) in AcOH (20 mL) were heated at 90 °C with stirring for 10 min and partitioned between EtOAc and saturated Na_2CO_3 solution, and the organic layer was separated, washed, and evaporated to dryness to give the crude aniline as a brownish residue. The crude residue was purified by triturating with Et_2O . This gave the aniline product **16** (518 mg, 60%); a further crop of product **16** could be recovered from the ethereal supernatant on standing if so desired. $M^+ [ES^+]$ 403, 405. 1H NMR (DMSO- d_6): δ 7.1–7.6 (9H, m), 6.23 (1H, d, $J = 9.2$ Hz), 6.04 (1H, s), 4.23 (2H, bs), 3.40 (2H, bs), 3.19 (4H, bs), 2.34 (4H, bs). Anal. found: C, 70.87; H, 6.08; N, 13.60; $C_{24}H_{23}ClN_4 \cdot 0.25H_2O$ requires C, 70.75; H, 5.81; N, 13.75%.

7-(4-(4'-Chlorobiphenyl-2-yl)methyl)piperazin-1-yl)quinazolin-4-amine (**17**). The aniline compound **16** (216 mg, 0.54 mmol) was on-reacted with formamidine acetate (194 mg, 3.24 mmol) in methyl glycol (5 mL) at reflux for 3 h under nitrogen, and the product was precipitated from the dark, cooled reaction mixture by the addition of a little water. This was filtered and dried to give the 4-aminoquinazoline **17** as a buff solid that could be recrystallized from aqueous DMSO after neutralization with aqueous ammonia (198 mg, yield 81%). $M^+ [ES^+]$ 430, 432. 1H NMR (DMSO- d_6): δ 8.18, (1H, s), 7.95 (1H, d, $J = 9.2$ Hz), 7.47–7.50 (1H, m), 7.45 (4H, bs), 7.29–7.36 (4H, m), 7.20–7.23 (1H, m), 7.16 (1H, dd, $J = 9.2$ and 2.4 Hz), 6.80 (1H, d, $J = 2.3$ Hz), 3.37 (2H, s), 3.23 (4H, m), 2.40 (4H, m). Anal. found: C, 68.26; H, 5.47; N, 15.54; $C_{25}H_{24}ClN_5 \cdot 0.5H_2O$ requires C, 69.84; H, 5.63; N, 16.29%.

7-(4-(4'-Chlorobiphenyl-2-yl)methyl)piperazin-1-yl)quinazolin-4-ol (**18**). The 4-aminoquinazoline compound **17** (176 mg, 0.4 mmol) was heated at 130 °C for 9 h in AcOH (2 mL) and 2.5 N HCl solution (2 mL) in a small flask fitted with an air condenser. The solvent was removed, and the residue was recrystallized from aqueous DMSO after neutralization with minimal aqueous ammonia. This gave the hydrolyzed product **18** as a buff powder (153 mg, 87% yield). HRESMS found: (M + H) 431.1636; $C_{25}H_{23}ClN_4O$ requires (M + H), 431.1633. 1H NMR (DMSO- d_6): δ 11.8 (1H, bs), 7.90 (1H, s), 7.84 (1H, d, $J = 9.0$ Hz), 7.46–7.51 (1H, m), 7.44 (4H, bs), 7.30–7.38 (2H, m), 7.20–7.23 (1H, m), 7.09 (1H, dd, $J = 9.0$ and 2.0 Hz), 6.86 (1H, d, $J = 2.0$ Hz), 4.44–3.37 (2H, bs), 3.27 (4H, m), 2.38 (4H, bm).

4-Chloro-7-(4-(4'-chlorobiphenyl-2-yl)methyl)piperazin-1-yl)quinazolin-4-ol (**19**). The hydrolyzed product **18** (30 mg, 0.07 mmol) was treated with dry $CHCl_3$ (1 mL) and $SOCl_2$ (1 mL) with a catalytic amount of DMF (10 μ L). The solution was then heated to reflux for 1 h, the solution was poured onto ice, and the product was extracted with EtOAc (2 \times 6 mL) to give the chlorinated product **19**, which was on-reacted without characterization.

N-{7-[4-(4'-Chloro-biphenyl-2-yl)methyl)piperazin-1-yl]quinazolin-4-yl}-4-((R)-3-dimethylamino-1-phenylsulfanylmethyl-propylamino)-3-nitro-benzenesulfonamide (**21**). A portion of the chlorinated product **19** (8 mg, 0.018 mmol), the sulfonamide **20** (8 mg, 0.018 mmol),¹⁵ and K_2CO_3 (40 mg, 0.288 mmol) in DMF (0.2 mL) was heated at 85 °C for 24 h. The reaction mixture was partitioned between EtOAc (2 mL) and water (2 mL). The organic layer was separated, dried ($MgSO_4$), and evaporated in vacuo to give a yellow residue. This residue was purified by HPLC to give of the quinazoline isostere **21** (2 mg, 13%) as a yellow glass.

tert-Butyl 4-(3-Amino-4-cyanophenyl)piperazine-1-carboxylate (**35**). A mixture of tert-butyl 4-(4-cyano-3-nitrophenyl)piperazine-1-carboxylate **12** (3 g, 9.9 mmol) and iron powder (2 g, 35.8 mmol) in AcOH (20 mL) was heated at 60 °C with rapid stirring. The reaction mixture was diluted with EtOAc (60 mL) and filtered twice through Celite. The filtrate was washed with a base wash using 6 N NaOH solution. The organic layer was then dried ($MgSO_4$) and concentrated

under vacuum to give the aniline **35** as a pale yellow powder (72%). 1H NMR ($CDCl_3$): δ 7.22 (1H, d, $J = 8.8$ Hz), 6.25 (1H, dd, $J = 2.1$ and 8.9 Hz), 6.09 (1H, d, $J = 2.3$ Hz), 4.33 (2H, bs), 3.55–3.51 (4H, m), 3.24–3.21 (4H, m), 1.46 (9H, s). Anal. found: C, 63.49; H, 7.24; N, 18.28; $C_{16}H_{22}N_4O_2$ requires C, 63.55; H, 7.33; N, 18.53%.

tert-Butyl 4-(4-Aminoquinazolin-7-yl)piperazine-1-carboxylate (**36**). tert-Butyl 4-(3-amino-4-cyanophenyl)piperazine-1-carboxylate **35** (1.5 g, 4.97 mmol) in methoxyethanol (10 mL) at 120 °C was treated portionwise every 1 h with formamidine acetate (4 \times 12.4 mmol). The mixture was heated at that temperature for a further 6 h. After standing for 20 h at room temperature, Et_2O (40 mL) was added. The resulting precipitate was filtered, washed with Et_2O , slurried with water (40 mL), and refiltered to afford the quinazoline **36** as a colorless powder (1.1 g, 69%). On standing, the filtrate after evaporation of the organic layer gave a further crop of crude product (22%). 1H NMR (DMSO- d_6): δ 8.23 (1H, s), 8.02 (1H, d, $J = 9.21$ Hz), 7.39 (2H, bs), 7.23 (1H, dd, $J = 2.6$ and 9.2 Hz), 6.88 (1H, d, $J = 2.5$ Hz), 3.50–3.46 (4H, m), 3.35–3.30 (4H, m), 1.43 (9H, s). Anal. found: C, 61.92; H, 6.83; N, 21.25; $C_{17}H_{23}N_5O_2$ requires C, 61.99; H, 7.04; N, 21.26%.

7-(Piperazin-1-yl)quinazolin-4-ol dihydrobromide (**24**). tert-Butyl 4-(4-aminoquinazolin-7-yl)piperazine-1-carboxylate **36** (1.3 g, 4 mmol) was then added carefully with rapid stirring (note that vigorous effervescence occurred) to 6 N hydrobromic acid (6 mL). Further stirring and heating at 130 °C occurred in a capped vessel for 3 h. After the hot reaction mixture was added to hot MeOH (50 mL), the whole was allowed to cool for 20 h. The precipitate that formed was filtered off to afford 7-(piperazin-1-yl)quinazolin-4-ol dihydrobromide **24** as colorless needles (1.5 g, 97%). $M^+ 231$. 1H NMR (DMSO- d_6): δ 8.87 (2H, bs), 8.61 (1H, bs), 7.98 (1H, d, $J = 9.0$ Hz), 7.01 (1H, d, $J = 2.4$ Hz), 3.71–3.61 (4H, m), 3.60–3.40 (4H, m). Anal. found: C, 34.29; H, 4.41; N, 13.24; $C_{12}H_{16}Br_2N_4O \cdot 1.5H_2O$ requires C, 34.39; H, 4.57; N, 13.37%.

7-[4-(4'-Chloro-biphenyl-2-yl)methyl)piperazin-1-yl]quinazolin-4-ol (**18**). DIPEA (384 μ L, 2.55 mmol) was added to a stirred solution of the 7-(piperazin-1-yl)quinazolin-4-ol dihydrobromide **24** (500 mg, 1.28 mmol) in DMF (10 mL). To this solution, 2-bromomethyl-4'-chlorobiphenyl **22** (X = Br) (360 mg, 1.28 mmol) in DMF (4 mL) was added dropwise over 30 min. The solution was allowed to stir at room temperature for 20 h. A solution of 10% $NaHCO_3$ (50 mL) was added to the stirred solution. The resulting precipitate was filtered off and dried in a vacuum oven to yield the quinazolinone **18** as a white solid (440 mg, 80%). The compound was of sufficient purity to be used in the next step without further purification. HRESMS found: (M + H) 431.1636; $C_{25}H_{23}ClN_4O$ requires (M + H), 431.1633. 1H NMR (DMSO- d_6): δ 7.92 (1H, s), 7.86 (1H, d, $J = 9.0$ Hz), 7.52–7.34 (7H, m), 7.23 (1H, dd, $J = 6.9$ and 1.9 Hz), 7.11 (1H, dd, $J = 9.0$ and 2.2 Hz), 6.88 (1H, d, $J = 2.3$ Hz), 3.38 (2H, s), 3.25 (4H, bs), and 2.41 (4H, bs). LCMS: Tr = 5.77 min, $m/z = 431$.

4-Chloro-7-[4-(4'-chloro-biphenyl-2-yl)methyl)piperazin-1-yl]quinazolin-4-ol (**19**). A solution of $POCl_3$ (0.5 mL) and DMF (2 drops) in 1,2-DCE (2 mL) was added dropwise over 15 min to a stirred solution of the 7-[4-(4'-chloro-biphenyl-2-yl)methyl)-piperazin-1-yl]-quinazolin-4-ol **37** (500 mg, 1.16 mmol) in 1,2-DCE (30 mL) at 70 °C under an atmosphere of nitrogen. Additional $POCl_3$ was added in increments (1 mL) of 15 min over 1 h. The solution was allowed to stir at 70 °C for 20 h. The solution was then concentrated in vacuo to dryness and then diluted with a solution of 10% $NaHCO_3$ (40 mL) and CH_2Cl_2 (40 mL). The layers were separated, and the organic layer was dried ($MgSO_4$) and concentrated in vacuo. The resulting residue was then applied to alumina column chromatography gradient eluting from 100% CH_2Cl_2 to 0.5% MeOH/ CH_2Cl_2 to afford the quinazoline **19** as a yellow foam (287 mg, 55%), which was on-reacted without characterization.

7-[4-[2-(4-Chloro-phenyl)-5,5-dimethyl-cyclohex-1-enylmethyl]-piperazin-1-yl]quinazolin-4-ol (**37**). DIPEA (384 μ L, 2.55 mmol) was

added to a stirred solution of the 7-(piperazin-1-yl)quinazolin-4-ol dihydrobromide **24** (500 mg, 1.28 mmol) in DMF (10 mL). To this solution, 1-(2-bromomethyl-4,4-dimethyl-cyclohex-1-enyl)-4-chlorobenzene **23** (X = Br) (401 mg, 1.28 mmol) in DMF (4 mL) was added dropwise over 30 min. The solution was allowed to stir at room temperature for 20 h. A solution of 10% NaHCO₃ (50 mL) was added to the stirred solution. The resulting precipitate was filtered off and dried in a vacuum oven to yield the quinazolinone **37** as a white solid (593 mg, 84%). The compound was of sufficient purity to be used in the next step without further purification. HRESMS found: (M + H) 463.2281; C₂₇H₃₁ClN₄O requires (M + H), 463.2259. ¹H NMR (DMSO-*d*₆): δ 7.92 (1H, s), 7.83 (1H, d, *J* = 9.0 Hz), 7.36 (2H, d, *J* = 6.5 Hz), 7.15 (2H, d, *J* = 6.5 Hz), 7.06 (1H, dd, *J* = 9.0 and 2.4 Hz), 6.82 (1H, d, *J* = 2.3 Hz), 3.25 (4H, bs), 2.74 (2H, bs), 2.27–2.21 (6H, m), 1.98 (2H, s), 1.42 (2H, t, *J* 6.4 Hz), and 0.96 (6H, s).

4-Chloro-7-{4-[2-(4-chloro-phenyl)-5,5-dimethyl-cyclohex-1-enylmethyl]piperazin-1-yl} (38). A solution of POCl₃ (0.5 mL) and DMF (2 drops) in 1,2-DCE (2 mL) was added dropwise over 15 min to a stirred solution of **37** (537 mg, 1.16 mmol) in 1,2-DCE (30 mL) at 70 °C under an atmosphere of nitrogen. Additional POCl₃ was added in increments (1 mL) of 15 min over 1 h. The solution was allowed to stir at 70 °C for 20 h. The solution was then concentrated in vacuo to dryness and then diluted with a solution of 10% NaHCO₃ (40 mL) and CH₂Cl₂ (40 mL). The layers were separated, and the organic layer was dried (MgSO₄) and concentrated in vacuo. The resulting residue was then applied to alumina column chromatography gradient eluting from 100% CH₂Cl₂ to 0.5% MeOH/CH₂Cl₂ to afford the quinazoline **38** as a yellow foam (324 mg, 58%), which was on-reacted without characterization.

N-{7-[4-(4'-Chloro-biphenyl-2-ylmethyl)piperazin-1-yl]quinazolin-4-yl}-4-((*R*)-3-dimethylamino-1-phenylsulfanylmethyl-propylamino)-3-nitro-benzenesulfonamide (21). A solution of the chloroquinazolinone **19** (100 mg, 0.22 mmol), the sulfonamide **20** (93 mg, 0.22 mmol), Cs₂CO₃ (101 mg, 0.31 mmol), Pd(PPh₃)₄ (2.5 mol %), and CuI (5.7 mg, 0.03 mmol) in dioxane (4 mL) was degassed for 5 min before being subjected to microwave irradiation (300 W, 150–180 °C, CEM Discover Labmate) for 45 min. The mixture was filtered washing with EtOAc and then washed with solution of 10% NaHCO₃ (10 mL). The organic layer was dried (MgSO₄) and concentrated in vacuo to give a crude residue. This residue was then subjected to preparative reverse phase HPLC for purification to afford the sulfonamide **21**. ¹H NMR (500 MHz, DMSO-*d*₆): δ 9.3–9.4 (m, 1H), 8.52 (s, 1H), 8.15–8.25 (m, 1H), 7.98–8.08 (m, 1H), 7.85 (d, *J* = 2.5 Hz, 1H), 7.45–7.55 (m, 4H), 7.35–7.45 (m, 4H), 7.25–7.35 (m, 1H), 7.20–7.30 (m, 4H), 7.05–7.15 (m, 4H), 4.1–4.2 (m, 2H), 3.05–3.15 (m, 4H), 2.72 (s, 6H), 2.11 (m, 2H). LCMS: Tr = 12.48 min, *m/z* = 837.

N-{7-[4-(4'-Chloro-biphenyl-2-ylmethyl)piperazin-1-yl]quinazolin-4-yl}-4-((*R*)-3-morpholin-4-yl-1-phenylsulfanylmethyl-propylamino)-3-nitro-benzenesulfonamide (28). Compound **28** was prepared from **25**¹⁵ and **19** following the procedure for **21**. ¹H NMR (500 MHz, DMSO-*d*₆): δ 9.6–9.7 (m, 1H), 8.52 (brs, 1H), 8.15–8.25 (m, 1H), 7.99–8.09 (m, 1H), 7.87 (d, *J* = 2.5 Hz, 1H), 7.45–7.55 (m, 4H), 7.35–7.45 (m, 2H), 7.28–7.38 (m, 1H), 7.20–7.30 (m, 4H), 7.05–7.15 (m, 5H), 4.1–4.15 (m, 1H), 3.85–4.00 (m, 2H), 3.35 (s, 6H), 3.12–3.28 (m, 4H), 2.98–3.08 (m, 2H), 2.10–2.20 (m, 2H). LCMS: Tr = 12.50 min, *m/z* = 879.

N-{7-[4-(4'-Chloro-biphenyl-2-ylmethyl)piperazin-1-yl]quinazolin-4-yl}-4-((*R*)-3-dimethylamino-1-phenylsulfanylmethyl-propylamino)-3-trifluoromethanesulfonyl-benzenesulfonamide (29). Compound **29** was prepared from **26**¹⁰ and **19** following the procedure for **21**. ¹H NMR (500 MHz, DMSO-*d*₆): δ 9.35–9.45 (m, 1H), 8.13–8.23 (m, 2H), 7.98 (d, *J* = 2.5 Hz, 2H), 7.50 (d, *J* = 2.0 Hz, 4H), 7.35–7.48 (m, 2H), 7.28 (d, *J* = 2.0 Hz, 4H), 7.25 (d, *J* = 2.5 Hz, 1H), 7.21 (t, *J* = 2 Hz, 2H), 7.10–7.18 (m, 1H), 6.98–7.08 (m, 1H), 6.75–6.85 (m, 1H), 4.00–4.05 (m,

2H), 3.10–3.15 (m, 2H), 3.03–3.08 (m, 2H), 2.71 (s, 6H), 2.0–2.1 (m, 2H). LCMS: Tr = 13.46 min, *m/z* = 924.

N-{7-[4-(4'-Chloro-biphenyl-2-ylmethyl)piperazin-1-yl]quinazolin-4-yl}-4-((*R*)-3-morpholin-4-yl-1-phenylsulfanylmethyl-propylamino)-3-trifluoromethanesulfonyl-benzenesulfonamide (30). Compound **30** was prepared from **27**¹⁰ and **19** following the procedure for **21**. ¹H NMR (500 MHz, DMSO-*d*₆): δ 9.65–9.75 (m, 1H), 8.18–8.32 (m, 2H), 8.02 (d, *J* = 2.5 Hz, 1H), 7.50–7.60 (m, 4H), 7.38–7.48 (m, 2H), 7.20–7.40 (m, 7H), 7.12–7.18 (m, 1H), 7.00–7.10 (m, 1H), 6.80–6.90 (m, 1H), 4.05–4.10 (m, 1H), 3.95–4.00 (m, 2H), 3.70 (s, 6H), 2.95–3.10 (m, 6H), 2.10–2.20 (m, 2H). LCMS: Tr = 5.57 min, *m/z* = 966.

N-{7-[4-[2-(4-Chloro-phenyl)-5,5-dimethyl-cyclohex-1-enylmethyl]piperazin-1-yl]quinazolin-4-yl}-4-((*R*)-3-dimethylamino-1-phenylsulfanylmethyl-propylamino)-3-nitro-benzenesulfonamide (31). Compound **31** was prepared from **20**¹⁵ and **38** following the procedure for **21**. ¹H NMR (500 MHz, DMSO-*d*₆): δ 9.32–9.42 (m, 2H), 8.50–8.52 (m, 1H), 8.14–8.24 (m, 2H), 7.98–8.08 (m, 1H), 7.86 (d, *J* = 2.5 Hz, 1H), 7.34–7.84 (m, 3H), 7.20–7.30 (m, 3H), 7.05–7.15 (m, 5H), 4.10–4.20 (m, 2H), 4.00–4.10 (m, 1H), 3.60–3.65 (m, 4H), 3.02–3.12 (m, 6H), 2.75–2.85 (m, 2H), 2.70 (s, 6H), 2.25–2.30 (m, 2H), 2.13 (q, *J* = 7 Hz, 2H), 2.01–2.10 (m, 2H), 1.45–1.50 (m, 2H), 1.00 (s, 6H). LCMS: Tr = 5.76 min, *m/z* = 869.

N-{7-[4-[2-(4-Chloro-phenyl)-5,5-dimethyl-cyclohex-1-enylmethyl]piperazin-1-yl]quinazolin-4-yl}-4-((*R*)-3-morpholin-4-yl-1-phenylsulfanylmethyl-propylamino)-3-nitro-benzenesulfonamide (32). Compound **32** was prepared from **25**¹⁵ and **38** following the procedure for **21**. ¹H NMR (500 MHz, DMSO-*d*₆): δ 9.52–9.62 (m, 1H), 9.28–9.38 (m, 1H), 8.52 (s, 1H), 8.14–8.24 (m, 2H), 7.98–8.08 (m, 1H), 7.83 (d, *J* = 2.5 Hz, 1H), 7.40 (d, *J* = 2 Hz, 2H), 7.20–7.30 (m, 3H), 7.05–7.15 (m, 6H), 4.10–4.20 (m, 2H), 3.91–4.02 (m, 4H), 3.52–3.58 (m, 6H), 3.12–3.22 (m, 2H), 2.95–3.05 (m, 2H), 2.80–2.90 (m, 2H), 2.25–2.30 (m, 2H), 2.12–2.18 (m, 2H), 2.01–2.06 (brs, 2H), 1.45–1.50 (m, 2H), 1.00 (s, 6H). LCMS: Tr = 14.12 min, *m/z* = 456.

N-{7-[4-[2-(4-Chloro-phenyl)-5,5-dimethyl-cyclohex-1-enylmethyl]piperazin-1-yl]quinazolin-4-yl}-4-((*R*)-3-dimethylamino-1-phenylsulfanylmethyl-propylamino)-3-trifluoromethanesulfonyl-benzenesulfonamide (33). Compound **33** was prepared from **26**¹⁰ and **38** following the procedure for **21**. ¹H NMR (500 MHz, DMSO-*d*₆): δ 9.35–9.45 (m, 2H), 8.15–8.25 (m, 2H), 7.98–8.06 (m, 2H), 7.42 (d, *J* = 2.5 Hz, 2H), 7.22–7.32 (m, 3H), 7.20–7.30 (m, 3H), 7.05–7.15 (m, 3H), 6.95–7.05 (m, 1H), 6.79–6.88 (m, 1H), 4.00–4.10 (m, 2H), 3.60–3.65 (m, 2H), 3.25–3.35 (m, 4H), 3.12–3.22 (m, 4H), 2.95–3.05 (m, 2H), 2.80–2.90 (m, 2H), 2.72 (s, 6H), 2.25–2.30 (m, 2H), 2.00–2.10 (m, 4H), 1.45–1.50 (m, 2H), 1.00 (s, 6H). LCMS: Tr = 14.93 min, *m/z* = 956.

N-{7-[4-[2-(4-Chloro-phenyl)-5,5-dimethyl-cyclohex-1-enylmethyl]piperazin-1-yl]quinazolin-4-yl}-4-((*R*)-3-morpholin-4-yl-1-phenylsulfanylmethyl-propylamino)-3-trifluoromethanesulfonyl-benzenesulfonamide (34). Compound **34** was prepared from **27**¹⁰ and **38** following the procedure for **21**. ¹H NMR (500 MHz, DMSO-*d*₆): δ 9.65–9.75 (m, 1H), 9.32–9.42 (m, 1H), 8.15–8.25 (m, 2H), 7.98–8.04 (m, 2H), 7.40 (d, *J* = 2 Hz, 1H), 7.29 (d, *J* = 2 Hz, 2H), 7.20–7.25 (m, 2H), 7.12–7.18 (m, 3H), 7.00–7.05 (m, 1H), 6.78–6.84 (m, 1H), 3.90–4.12 (m, 4H), 3.31–3.41 (m, 6H), 3.15–3.25 (m, 2H), 2.95–3.15 (m, 4H), 2.80–2.90 (m, 2H), 2.25–2.30 (m, 2H), 2.00–2.15 (m, 4H), 1.45–1.50 (m, 2H), 1.00 (s, 6H). LCMS: Tr = 15.02 min, *m/z* = 998.

AlphaSCREEN Assay. AlphaSCREEN is a bead-based technology, which facilitates the measurement of the interaction between molecules. The assay consisted of two hydrogel-coated beads, which when brought into close proximity by a binding interaction allow the transfer of singlet oxygen from a donor bead to an acceptor bead. Upon binding and excitation with laser light at 680 nm, a photosensitizer in the donor bead converts ambient oxygen to a more excited singlet state. This singlet oxygen then diffuses across to react with a chemiluminescer in the acceptor bead. Fluorophores within the same bead are activated, resulting

in the emission of light at 580–620 nm. Screening of the test compounds was performed using the AlphaSCREEN GST (glutathione S-transferase) detection kit system (Perkin-Elmer Lifesciences). Briefly, test compounds were titrated into the assay, which consisted of GST-tagged Bcl-x_L ΔC25 protein (0.6 nM final concentration) and biotinylated Bim BH3–26 peptide, Biotin-DLRPEIRIAQELRRIGDEFNETYTRR (5.0 nM final concentration), anti-GST-coated acceptor beads, and streptavidin-coated donor beads (both bead types at a final concentration of 15 μg/mL) and a room temperature incubation time of 4 h before reading. More specifically, (i) a 384 well-plate was prepared with 4.75 μL of buffer and 0.25 μL of compound stock (20 mM in DMSO) per well; (ii) binding partners were mixed—in one tube, Bcl-x_L was added with the acceptor beads, while in the second tube biotinylated BH3 peptide was added with the donor beads; (iii) these two pairs of binding partners were pre-incubated for 30 min; (iv) 10 μL of the acceptor beads/Bcl-x_L protein complex was then added to each of the 384 wells; (v) plates were sealed and incubated at room temperature for a further 30 min; (vi) 10 μL of the donor bead/BH3 peptide complex was then added to each of the 384 wells; (vii) plates were sealed, covered with foil, and incubated for a further 4 h and then read. The assay buffer contained 50 mM HEPES, pH 7.4, 10 mM DTT, 100 mM NaCl, 0.05% Tween 20, and 0.1 mg/mL casein. Bead dilution buffer contained 50 mM Tris-HCl, pH 7.5, 0.01% Tween 20, and 0.1 mg/mL casein. The final DMSO concentration in the assay was 1.0% (v/v). Assays were performed in 384-well white Opti-plates (Perkin-Elmer Lifesciences) and analyzed on the PerkinElmer Fusion Alpha plate reader (Ex680, Em520–620 nm).

Determination of Binding Affinity by Biacore S51 SPR Analysis. *Immobilization of anti-GST Antibody.* Anti-GST antibody surfaces were prepared by using standard amine-coupling procedures as instructed by the GST Capture Kit from Biacore. The running buffer was 10 mM NaH₂PO₄·H₂O, 40 mM Na₂HPO₄·2H₂O, 150 mM NaCl, 1.0 mM EDTA, 0.03% Tween 20, and 5% DMSO, pH 7.4. Flow cells (spots) were activated by injecting 200 μL of (11.5 mg/mL) NHS and (75 mg/mL) EDC. Fifty microliters of (30 μg/mL) anti-GST antibody in 10 mM sodium acetate, pH 5.0, was injected for 10 min at 5 μL/min, followed by the injection of 175 μL of ethanolamine (1 M). This was followed by the injection for 36 s of Biadesorb1 solution (0.5% SDS) and 40 s of Biadesorb2 solution (50 mM glycine, pH 9.5) at 30 μL/min at the end of the run. These methods resulted consistently in about 10000 RU anti-GST antibody immobilized over separate experiments.

Capture of GST-Bcl-x_L. The running buffer was the same as used for the immobilization of anti-GST antibody. GST-Bcl-x_L (0.1–0.2 mg/mL) in the running buffer was injected at 10 μL/min for 3 min across one spot, resulting in the capture of approximately 1200 RU protein.

Kinetic Analysis of Small Molecules and GST-Bcl-x_L Interactions. A concentration series of each compound was injected at a flow rate of 90 μL/min over three spots (one spot was immobilized with GST-Bcl-x_L protein capture by anti-GST antibody, the other two spots were free) at 25 °C. The association time and dissociation time were 95 and 240 s, respectively. The buffer blanks were also injected periodically for double referencing. The buffer samples containing 4–6% DMSO were injected for solvent correction. The antibody surface was regenerated between binding cycles with 40 s injection of 10 mM glycine-HCl, pH 2.2, and 40 s injection of 0.05% SDS. Fresh protein was injected at 10 μL/min for 3 min at the beginning of each binding cycle.

Data Analysis. All sensorgram data were processed by using double referencing. Thus, first the response from the reference spot (no immobilization) was subtracted from the binding response obtained on the test spot followed by solvent correction (to correct for DMSO bulk shift responses). Then, the response from an average of buffer injections was also subtracted from the remaining response 1 described above to obtain final corrected response units. To obtain kinetic rate constants (k_a and k_d), corrected response data were then fit to a one-to-

one binding site model, which includes mass transport limitations. The equilibrium dissociation constant (K_D) was determined by k_d/k_a .

Determination of Selectivity Profile by Biacore S3000 SPR Analysis. *Recombinant Proteins.* Expression and purification of the loop-deleted form of human Bcl-x_L (Δ27–82, ΔC24) for crystallization and Bcl-2 ΔC22, Bcl-x_L ΔC24, Bcl-w C29S/A128E ΔC29, and human/mouse chimeric Mcl-1 (ΔN170, ΔC23) for Biacore studies was performed as described previously.^{21–23}

Binding Affinity Measurements—Solution Competition Assays. Solution competition assays were performed using a Biacore 3000 instrument as described previously.²⁴ Briefly, pro-survival proteins (10 nM) were incubated with varying concentrations of compounds for at least 2 h in running buffer [10 mM HEPES, 150 mM NaCl, 3.4 mM EDTA, and 0.005% (v/v) Tween 20, pH 7.4] prior to injection onto a CM5 sensor chip on which either a wild-type mBimBH3 (DLRPEIRIAQELRRIGDEFNETYTRR) peptide or an inert mBimBH3 (DLRPEIRIAQEERREGDEENETYTRR) mutant peptide was immobilized. Specific binding of the pro-survival protein to the surface in the presence and absence of compounds was quantified by subtracting the signal from the Bim mutant channel from that obtained on the wild-type Bim channel. The IC₅₀ was calculated by nonlinear curve fitting of the data with Kaleidagraph (Synergy Software).

X-ray Structural Data. Crystallization was performed as previously described for the Bcl-x_L:1 complex.¹⁶ Briefly, Bcl-x_L was combined with compound 21 at equimolar concentrations, the complex was concentrated to 10 mg/mL, and crystals were grown in hanging drops at 295 K with a reservoir solution consisting of 1.1 M sodium citrate and 0.1 M Tris, pH 8.0. Crystals were soaked for 30 s in cryoprotectant (1.1 M sodium citrate, 0.1 M Tris, pH 8.0, 5% DMSO, and 12.5% glycerol) and flash frozen in liquid nitrogen. X-ray data were collected at 100 K using an in-house RAXIS-IV++ detector with a micro-max007 rotating anode X-ray source. Data were integrated and scaled with HKL2000.²⁵ The R-free set from the data used to solve the 1:Bcl-x_L structure was transferred to the new data to avoid model bias. The structure was solved by performing Rigid Body refinement with REFMAC5²⁶ using the Bcl-x_L coordinates from the Bcl-x_L:1 complex (2YXJ) as a starting model. Several rounds of building in COOT²⁷ and refinement with REFMAC5 led to the model described in the Supporting Information.

MEF Viability Assay. MEFs were maintained in high-glucose DME supplemented with 250 mM L-asparagine, 50 mM 2-mercaptoethanol, and 10% (v/v) FCS (Bovagen). Cells were exposed to compounds at the indicated concentrations for 24 h in medium containing 1 or 10% FCS. The cytotoxicity was assessed with CellTiter Glo (Promega).

SCLC Viability Assay. *Cell Culture.* The SCLC cell lines NCI-H889, NCI-H1963, and NCI-H146 were purchased from the American Type Culture Collection (Manassas, VA). Cells were cultured in RPMI 1640 (Invitrogen Corp., Grand Island, NY) supplemented with 10% fetal bovine serum (Invitrogen), 1% sodium pyruvate, 25 mmol/L HEPES, 4.5 g/L glucose, and 1% penicillin/streptomycin (Sigma). All cell lines were maintained in a humidified chamber at 37 °C containing 5% CO₂.

Cell Treatment and Viability Assays. Cells were treated for 48 h in 96-well tissue culture plates in a total volume of 100 μL of tissue culture medium supplemented with 10% human serum (Invitrogen). Each concentration was tested in duplicate at least thrice separately. Viable cells were determined using the CellTiter 96 AQueous nonradioactive cell proliferation MTS assay (Promega Corp., Madison, WI).

■ ASSOCIATED CONTENT

§ **Supporting Information.** Supplementary Table 1, Crystallographic statistics. This material is available free of charge via the Internet at <http://pubs.acs.org>.

Accession Codes

The PDB ID is 3QKD.

■ AUTHOR INFORMATION

Corresponding Author

*Tel: +61 3 9345 2108. Fax: +61 3 9345 2100. E-mail: jbaell@wehi.edu.au.

■ ACKNOWLEDGMENT

This work was supported by Fellowships and Grants from the Leukemia and Lymphoma Society (SCOR 7015-02). Crystallization trials were performed at the Bio21 Collaborative Crystallisation Centre, Victoria, Australia. We thank Peter Colman for useful discussions and also the NHMRC, the Victorian State Government, the Cancer Council of Victoria, the Australian Cancer Research Foundation, and the Australian Research Council for the following support: NHMRC Program Grant 461221; NHMRC IRISS Grant #361646; Victorian State Government OIS grant; Cancer Council of Victoria, Fraser Fellowship to P. M. Colman (2002–2006); ACRF Equipment Grant (2002); ARC Future Fellowship; and NHMRC Project Grant 575561 to P.E.C.

■ ABBREVIATIONS USED

AlphaSCREEN, amplified luminescent proximity homogeneous assay; A1, B-cell lymphoma 2 related protein A1; Bad, Bcl-2-associated death promotor; Bak, Bcl-2 antagonist/killer; Bax, Bcl-2 associated protein X; Bcl-2, B-cell lymphoma 2; Bcl-w, B-cell lymphoma w; Bcl-x_L, B-cell lymphoma extra long; BH, Bcl homology; Bid, BH3 interacting death domain; Bik, Bcl-2 interacting killer; Bim, Bcl-2 interacting mediator; Bmf, Bcl-2 modifying factor; Hrk, Harakiri-Bcl-2 interacting protein; Mcl-1, myeloid cell leukemia 1; MEF, mouse embryonic fibroblast; Noxa, phorbol-12-myristate-13-acetate-induced protein 1; Puma, Bcl-2 binding component 3; SCLC, small cell lung carcinoma; SPR, surface plasmon resonance

■ REFERENCES

- (1) Cory, S.; Adams, J. M. Killing cancer cells by flipping the Bcl-2/Bax switch. *Cancer Cell* **2005**, *8*, 5–6.
- (2) Hinds, M. G.; Smits, C.; Fredericks-Short, R.; Risk, J. M.; Bailey, M.; Huang, D. C. S.; Day, C. L. Bim, Bad and Bmf: Intrinsically unstructured BH3-only proteins that undergo a localized conformational change upon binding to prosurvival Bcl-2 targets. *Cell Death Differ.* **2007**, *14*, 128–136.
- (3) Hanahan, D.; Weinberg, R. A. The hallmarks of cancer. *Cell* **2000**, *100*, 57–70.
- (4) Adams, J. M.; Cory, S. The Bcl-2 apoptotic switch in cancer development and therapy. *Oncogene* **2007**, *26*, 1324–1337.
- (5) Labi, V.; Erlacher, M.; Kiessling, S.; Villunger, A. BH3-only proteins in cell death initiation, malignant disease and anticancer therapy. *Cell Death Differ.* **2006**, *13*, 1325–1338.
- (6) Lessene, G.; Czabotar, P. E.; Colman, P. M. Bcl-2 family antagonists for cancer therapy. *Nat. Rev. Drug Discovery* **2008**, *7*, 989–1000.
- (7) Baell, J. B.; Huang, D. C. S. Prospects for targeting the Bcl-2 family of proteins to develop novel cytotoxic drugs. *Biochem. Pharmacol.* **2002**, *64*, 851–863.
- (8) (a) van Delft, M. F.; Huang, D. C. S. How the Bcl-2 family of proteins interact to regulate apoptosis. *Cell Res.* **2006**, *16*, 203–213. (b) The descriptor “BH3 mimetics” is somewhat misleading. Over a decade ago, Ripka and Rich²⁸ attempted to clarify terminology in peptidomimetic research and delineated between type II mimetics and type III mimetics. The former is a nonpeptide that is a functional mimetic and that binds to a peptide binding site but does not do so in a way that represents topographical mimicry of the native binding epitope. The latter is a topographical mimetic of the native binding epitope even though superficially it may be hard to envisage any resemblance between the two. The field of BH3 mimetics comprises both type II and type III peptidomimetics. We find this distinction useful. Despite this, the proposed classification of peptidomimetics of Ripka and Rich does not appear to have been widely taken up.
- (9) Oltsersdorf, T.; Elmore, S. W.; Shoemaker, A. R.; Armstrong, R. C.; Augeri, D. J.; Belli, B. A.; Bruncko, M.; Deckwerth, T. L.; Dinges, J.; Hajduk, P. J.; Joseph, M. K.; Kitada, S.; Korsmeyer, S. J.; Kunzer, A. R.; Letai, A.; Li, C.; Mitten, M. J.; Nettesheim, D. G.; Ng, S.; Nimmer, P. M.; O'Connor, J. M.; Oleksijew, A.; Petros, A. M.; Reed, J. C.; Shen, W.; Tahir, S. K.; Thompson, C. B.; Tomaselli, K. J.; Wang, B.; Wendt, M. D.; Zhang, H.; Fesik, S. W.; Rosenberg, S. H. An inhibitor of Bcl-2 family proteins induces regression of solid tumours. *Nature* **2005**, *435*, 677–681.
- (10) Park, C. M.; Bruncko, M.; Adickes, J.; Bauch, J.; Ding, H.; Kunzer, A.; Marsh, K. C.; Nimmer, P.; Shoemaker, A. R.; Song, X.; Tahir, S. K.; Tse, C.; Wang, X.; Wendt, M. D.; Yang, X.; Zhang, H.; Fesik, S. W.; Rosenberg, S. H.; Elmore, S. W. Discovery of an Orally Bioavailable Small-molecule Inhibitor of Prosurvival B-Cell Lymphoma 2 Proteins. *J. Med. Chem.* **2008**, *51*, 6902–6915.
- (11) (a) Tse, C.; Shoemaker, A. R.; Adickes, J.; Anderson, M. G.; Chen, J.; Jin, S.; Johnson, E. F.; Marsh, K. C.; Mitten, M. J.; Nimmer, P.; Roberts, L.; Tahir, S. K.; Xiao, Y.; Yang, X.; Zhang, H.; Fesik, S.; Rosenberg, S. H.; Elmore, S. W. ABT-263: A potent and orally bioavailable Bcl-2 family inhibitor. *Cancer Res.* **2008**, *68*, 3421–3428. (b) More recent progress in phase II trials can be found at <http://clinicaltrials.gov> and by searching on “Navitoclax” (or “ABT-263”) and “phase II”.
- (12) Huang, S.; Connolly, P. J.; Lin, R.; Emanuel, S.; Middleton, S. A. Synthesis and evaluation of N-acyl sulfonamides as potential prodrugs of cyclin-dependent kinase inhibitor JNJ-7706621. *Bioorg. Med. Chem. Lett.* **2006**, *16*, 3639–3641.
- (13) Petros, A.; Dinges, J.; Augeri, D.; Baumeister, S.; Betebenner, D.; Bures, M. G.; Elmore, S. W.; Hajduk, P. J.; Joseph, M. K.; Landis, S. K.; Nettesheim, D. G.; Rosenberg, S. H.; Shen, W.; Thomas, S.; Wang, X.; Zanze, I.; Zhang, H.; Fesik, S. W. Discovery of a potent inhibitor of the antiapoptotic protein Bcl-x_L from NMR and parallel synthesis. *J. Med. Chem.* **2006**, *49*, 656–663.
- (14) Alternative coupling procedures involving attempted EDC/DMAP coupling between the hydroxyquinazoline and the sulfonamide, or from sulfonylation of the 4-aminoquinazoline with the sulfonyl chloride, were all unsuccessful.
- (15) Wendt, M. D.; Shen, W.; Kunzer, A.; McClellan, W. J.; Bruncko, M.; Oost, T. K.; Ding, H.; Joseph, M. K.; Zhang, H.; Nimmer, P. M.; Ng, S. C.; Shoemaker, A. R.; Petros, A. M.; Oleksijew, A.; Marsh, K.; Bauch, J.; Oltsersdorf, T.; Belli, B. A.; Martineau, D.; Fesik, S. W.; Rosenberg, S. H.; Elmore, S. W. Discovery and Structure Activity Relationship of Antagonists of B-Cell Lymphoma 2 Family Proteins with Chemopotentiation Activity in Vitro and in Vivo. *J. Med. Chem.* **2006**, *49*, 1165–1181.
- (16) Lee, E. F.; Czabotar, P. E.; Smith, B. J.; Deshayes, K.; Zobel, K.; Colman, P. M.; Fairlie, W. D. Crystal structure of ABT-737 complexed with Bcl-x_L: implications for selectivity of antagonists of the Bcl-2 family. *Cell Death Differ.* **2007**, *14*, 1711–1713.
- (17) Willis, S. N.; Chen, L.; Dewson, G.; Wei, A.; Naik, E.; Fletcher, J. I.; Adams, J. M.; Huang, D. C. S. Proapoptotic Bak is sequestered by Mcl-1 and Bcl-x_L, but not Bcl-2, until displaced by BH3-only proteins. *Genes Dev.* **2005**, *19*, 1294–1305.
- (18) Bruncko, M.; Oost, T. K.; Belli, B. A.; Ding, H.; Joseph, M. K.; Kunzer, A.; Martineau, D.; McClellan, W. J.; Mitten, M.; Ng, S. C.; Nimmer, P. M.; Oltsersdorf, T.; Park, C. M.; Petros, A. M.; Shoemaker, A. R.; Song, X.; Wang, X.; Wendt, M. D.; Zhang, H.; Fesik, S. W.; Rosenberg, S. H.; Elmore, S. W. Studies Leading to Potent, Dual Inhibitors of Bcl-2 and Bcl-x_L. *J. Med. Chem.* **2007**, *50*, 641–662.
- (19) A final difference is that the structural modification and optimization of ABT-737 en route to ABT-263, which conferred improved bioavailability to the latter compound, did not have the same

effect on the quinazoline sulfonamide system. Indeed, we undertook extensive pharmacokinetic analysis of all of the quinazolines reported herein and found that the oral bioavailability was low (<5%, data not shown). Both cell-based activity and pharmacokinetic behavior would therefore be the key parameters to improve in future medicinal chemistry optimization for the quinazoline sulfonamides.

(20) Baleizão, C.; Corma, A.; García, H.; Leyva, A. Oxime carbapalladacycle covalently anchored to high surface area inorganic supports or polymers as heterogeneous green catalysts for the Suzuki reaction in water. *J. Org. Chem.* **2004**, *69*, 439–446.

(21) Chen, L.; Willis, S. N.; Wei, A.; Smith, B. J.; Fletcher, J. L.; Hinds, M. G.; Colman, P. M.; Day, C. L.; Adams, J. M.; Huang, D. C. S. Differential targeting of prosurvival Bcl-2 proteins by their BH3-only ligands allows complementary apoptotic function. *Mol. Cell* **2005**, *17*, 393–403.

(22) Czabotar, P. E.; Lee, E. F.; van Delft, M. F.; Day, C. L.; Smith, B. J.; Huang, D. C. S.; Fairlie, W. D.; Hinds, M. G.; Colman, P. M. Structural insights into the degradation of Mcl-1 induced by BH3 domains. *Proc. Natl. Acad. Sci. U.S.A.* **2007**, *104*, 6217–6222.

(23) Lee, E. F.; Czabotar, P. E.; van Delft, M. F.; Michalak, E. M.; Boyle, M. J.; Willis, S. N.; Puthalakath, H.; Bouillet, P.; Colman, P. M.; Huang, D. C. S.; Fairlie, W. D. A novel BH3 ligand that selectively targets Mcl-1 reveals that apoptosis can proceed without Mcl-1 degradation. *J. Cell Biol.* **2008**, *180*, 341–355.

(24) Lee, E. F.; Fedorova, A.; Zobel, K.; Boyle, M. J.; Yang, H.; Perugini, M. A.; Colman, P. M.; Huang, D. C. S.; Deshayes, K.; Fairlie, W. D. Novel Bcl-2 homology-3 domain-like sequences identified from screening randomized peptide libraries for inhibitors of the pro-survival Bcl-2 proteins. *J. Biol. Chem.* **2009**, *284*, 31315–31326.

(25) Otwinowski, Z.; Minor, W. Processing of X-Ray Diffraction Data Collected in Oscillation Mode. *Methods Enzymol.* **1997**, *276*, 307.

(26) Murshudov, G. G.; Vagin, A. A.; Dodson, E. J. Refinement of macromolecular structures by the maximum-likelihood method. *Acta Crystallogr.* **1997**, *D53*, 240–255.

(27) Emsley, P.; Cowtan, K. Coot: Model-building tools for molecular graphics. *Acta Crystallogr.* **2004**, *D60*, 2126–2132.

(28) Ripka, A. S.; Rich, D. H. Peptidomimetic Design. *Curr. Opin. Chem. Biol.* **1998**, *2*, 441–452.

■ NOTE ADDED AFTER ASAP PUBLICATION

Bcl-x_L was defined incorrectly in the version of this paper published on March 2, 2011. The corrected version posted to the web on March 17, 2011.